Roles of Tyrosine 158 and Lysine 165 in the Catalytic Mechanism of InhA, the Enoyl−ACP Reductase from Mycobacterium tuberculosis †

ARTICLE *in* BIOCHEMISTRY · NOVEMBER 1999

Impact Factor: 3.02 · DOI: 10.1021/bi990529c · Source: PubMed

4 AUTHORS, INCLUDING:

Guqing Xiao

73 PUBLICATIONS **2,086** CITATIONS

SEE PROFILE

Peter J Tonge

Stony Brook University

196 PUBLICATIONS **4,403** CITATIONS

SEE PROFILE

Roles of Tyrosine 158 and Lysine 165 in the Catalytic Mechanism of InhA, the Enoyl-ACP Reductase from *Mycobacterium tuberculosis*†

Sapan Parikh,‡ Daniel P. Moynihan,‡,§ Guoping Xiao,‡ and Peter J. Tonge*,‡,||

Department of Chemistry, State University of New York at Stony Brook, Stony Brook, New York 11794-3400, and Graduate Program in Biophysics and Graduate Program in Molecular and Cellular Biochemistry, State University of New York at Stony Brook, Stony Brook, New York 11794

Received March 5, 1999; Revised Manuscript Received August 16, 1999

ABSTRACT: The role of tyrosine 158 (Y158) and lysine 165 (K165) in the catalytic mechanism of InhA, the enoyl-ACP reductase from *Mycobacterium tuberculosis*, has been investigated. These residues have been identified as putative catalytic residues on the basis of structural and sequence homology with the short chain alcohol dehydrogenase family of enzymes. Replacement of Y158 with phenylalanine (Y158F) and with alanine (Y158A) results in 24- and 1500-fold decreases in k_{cat}, respectively, while leaving K_m for the substrate, *trans*-2-dodecenoyl-CoA, unaffected. Remarkably, however, replacement of Y158 with serine (Y158S) results in an enzyme with wild-type activity. Kinetic isotope effect studies indicate that the transfer of a solvent-exchangeable proton is partially rate-limiting for the wild-type and Y158S enzymes, but not for the Y158A enzyme. These data indicate that Y158 does not function formally as a proton donor in the reaction but likely functions as an electrophilic catalyst, stabilizing the transition state for hydride transfer by hydrogen bonding to the substrate carbonyl. A conformational change involving rotation of the Y158 side chain upon binding of the enoyl substrate to the enzyme is proposed as an explanation for the inverse solvent isotope effect observed on V/K_{DD-CoA} when either NADH or NADD is used as the reductant. These data are consistent with the recently published structure of a C16 fatty acid substrate bound to InhA that shows Y158 hydrogen bonded to the substrate carbonyl group and rotated from the position it occupies in the InhA−NADH binary complex [Rozwarski, D. A., Vilcheze, C., Sugantino, M., Bittman, R., and Sacchettini, J. C. (1999) *J. Biol. Chem. 274*, 15582−15589]. Finally, the role of K165 has been analyzed using site-directed mutagenesis. Replacement of K165 with glutamine (K165Q) and arginine (K165R) has no effect on the enzyme's catalytic ability or on its ability to bind NADH. However, the K165A and K165M enzymes are unable to bind NADH, indicating that K165 has a primary role in cofactor binding.

InhA,[1] the enoyl-ACP reductase from *Mycobacterium tuberculosis*, catalyzes the NADH-dependent reduction of long chain *trans*-2-enoyl-ACP fatty acids (Scheme 1) and is a component of the mycobacterial fatty acid elongation cycle (*2*, *3*). The enzyme is inhibited by the anti-tubercular drug isoniazid (Scheme 1), consistent with the knowledge that isoniazid interferes with the biosynthesis of mycolic acids, long chain fatty acid components of the mycobacterial cell wall (*4*−*6*). Mutations in the structural gene for InhA are associated with isoniazid resistance in vivo, and currently, five InhA mutations have been observed in clinical isolates of isoniazid-resistant *M. tuberculosis*: I16T, I21V, I47T, V78A, and I95P (*7*). The drug-resistant InhA enzymes have a reduced affinity for NADH (*7*), consistent with the observation that an isoniazid metabolite covalently modifies the nicotinamide headgroup when NADH is bound to the enzyme (*6*).

Scheme 1

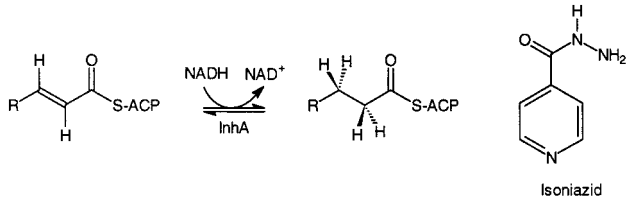

It is estimated that one-third of the world's population is infected with *M. tuberculosis* and that each year 3 million people die from tuberculosis (*8*). Consequently, tuberculosis

† This work was supported by a grant from the New York State Science and Technology Foundation and by NIH Grant AI40982 to P.J.T. S.P. is a DOE/GAANN Fellow. The NMR facility at the State University of New York at Stony Brook is supported by grants from the NSF (CHE8911350 and CHE9413510) and from the NIH (1S10RR554701). MALDI-MS data were collected at the Center for Analysis and Synthesis of Macromolecules at the State University of New York at Stony Brook, which is supported by NIH Grant RR02427 and the Center for Biotechnology.

* To whom correspondence should be addressed. E-mail: Peter.Tonge@sunysb.edu.

‡ Department of Chemistry.

§ Present address: Medical Program, Albert Einstein College of Medicine, Bronx, NY 10461.

|| Graduate Program in Biophysics and Graduate Program in Molecular and Cellular Biochemistry.

[1] Abbreviations: DD-CoA, *trans*-2-dodecenoyl-CoA; CoA, coenzyme A (lithium salt); DTNB, 5,5′-dithiobis(2-nitrobenzoic acid); SCAD family, short chain alcohol dehydrogenase family; AKR family, aldo-keto reductase family; 3αHSD, 3-α-hydroxysteroid dehydrogenase; InhA, enoyl-ACP reductase from *M. tuberculosis*; EnvM, enoyl-ACP reductase from *Escherichia coli* and *Brassica napus*.

10.1021/bi990529c CCC: $18.00
Published on Web 09/23/1999

is the leading cause of death of young people and adults in the world (*9*). A major factor in the increase in tuberculosis has been the spread of the AIDS epidemic, and currently, tuberculosis is one of the most common opportunistic infections in people with AIDS (*10*). Additionally, an important aspect of the disease concerns the increasing occurrence of multidrug-resistant strains of *M. tuberculosis*, with about 90% of the drug-resistant strains occurring in people infected with HIV (*11*, *12*). There is thus a critical need for the development of novel anti-tubercular drugs that are effective against drug-resistant strains of the organism.

As part of our effort to develop novel anti-tubercular drugs, we are studying the catalytic mechanism of InhA and identifying amino acid residues involved in catalysis. Here we report site-directed mutagenesis studies on two amino acids, Y158 and K165, that have been identified by sequence homology modeling as putative catalytic residues. These two residues are conserved within the enoyl-reductase family and are structurally homologous to conserved tyrosine and lysine residues in the short chain alcohol dehydrogenase (SCAD) family of enzymes (*13*, *14*). On the basis of the X-ray structure of EnvM, the enoyl-reductase from *Escherichia coli*, and mechanistic studies of SCAD enzymes, it has been proposed that the conserved tyrosine (Y156), possibly with assistance from the conserved lysine (K163), stabilizes the enolate intermediate by protonation (*13*, *14*).

In the X-ray structure of the InhA−NADH binary complex (*15*), Y158 and K165 cannot simultaneously interact with the substrate carbonyl due to an 86° rotation of the Y158 $C_\alpha-C_\beta$ bond relative to its position in EnvM (−153° in EnvM and −67° in InhA). On the basis of the InhA structure, Blanchard and co-workers have proposed that K165 is the electrophile that interacts with the substrate's carbonyl group (*16*). Our initial modeling studies indicate that the substrate carbonyl can also hydrogen bond with Y158, but this requires a major reorientation of the substrate in the active site relative to the model proposed by Blanchard et al. Alternatively, substrate binding could cause the tyrosine side chain to rotate and take up a position similar to that observed in EnvM.

To investigate the role that Y158 and K165 play in the reaction mechanism, Y158 has been replaced by S, F, and A while K165 has been replaced by R, M, Q, and A. The effect of the various replacements has been investigated using steady state kinetics and primary kinetic isotope effects. The data indicate that Y158 is involved in the chemical steps of the reduction reaction while the primary function of K165 is in cofactor binding. Our results are discussed in light of the recently published X-ray structure of InhA in complex with NAD^+ and a C16 fatty acid substrate reported by Sacchettini and co-workers (*1*). In this structure, Y158 has moved from its position in the binary InhA−NADH complex and hydrogen bonds with the substrate carbonyl.

EXPERIMENTAL PROCEDURES

Materials. Coenzyme A (CoA) lithium salt, β-NADH, β-NAD, glucose-6-phosphate dehydrogenase from *Leuconostoc mesenteroides* (type XXIV), and ethyl chloroformate were from Sigma Chemical Co. (St. Louis, MO). Triethylamine was from Aldrich (Milwaukee, WI). *trans*-2-Dodecenoic acid was from TCI Chemicals (Portland, OR). [1-D]-Glucose (98% D) and deuterium oxide (99.9% D) were purchased from Cambridge Isotope Labs (Andover, MA). Sephadex G-25 (fine) was purchased from Pharmacia Biotech (Uppsala, Sweden). His-Bind Resin, biotinylated thrombin, streptavidin−agarose, and the pET15(b) plasmid were purchased from Novagen (Madison, WI). Oligonucleotides were purchased from IDT, Inc. (Coralville, IA). Restriction enzymes (*Nde*I and *Bam*HI) were purchased from Stratagene (La Jolla, CA). T4 ligase, calf intestinal alkaline phosphatase (CIP), and T7 cloned *pfu* polymerase were purchased from New England Biolabs Inc. (Beverly, MA). Spin columns were purchased from Princeton Separations Inc. (Adelphia, NJ). DNA purification and gel extraction kits were from Qiagen Inc. (Valencia, CA). TSP-d_4 was purchased from Isotec Inc. (Miamisburg, OH). All other buffer salts (reagent grade or better), solvents (HPLC grade or better), and chemicals were purchased from Fisher Scientific Co. (Pittsburgh, PA).

Preparation of trans-2-Dodecenoyl-Coenzyme A. *trans*-2-Dodecenoyl-CoA (DD-CoA) was synthesized from *trans*-2-dodecenoic acid using the mixed anhydride method as described previously (*3*). Briefly, 50 mg (252 μmol) of acid was dissolved in 10 mL of anhydrous diethyl ether with 32 mg (315 μmol) of triethylamine. Following the addition of 34 mg (315 μmol) of ethyl chloroformate, salt crystals formed and the solution was stirred at room temperature overnight. The mixed anhydride was then filtered and added dropwise to a solution of CoA in 50 mM Na_2CO_3 (pH 8), ethanol, and ethyl acetate (1:1:1) while being stirred at room temperature. The reaction progress was monitored by following the concentration of free thiol in solution using 5,5′-dithiobis(2-nitrobenzoic acid) (DTNB). When no free thiol was detected, the solution was concentrated in vacuo to remove the organic solvent and was purified by HPLC (Shimadzu) using a Phenomenex Primesphere 5 C_{18}-HC 250 mm × 4.60 mm (5 μm) preparative column. Chromatography was performed using 20 mM ammonium acetate/1.75% acetonitrile as buffer A and running a 0 to 100% gradient of 95% acetonitrile/5% H_2O (buffer B) over the course of 80 min at a flow rate of 8 mL/min. Elution was monitored at 260 and 285 nm using a Shimadzu SPD-10A UV−vis detector, and fractions containing DD-CoA were pooled and lyophilized. The retention time for DD-CoA was 40 min. To remove all ammonium acetate, the lyophilized solid was redissolved in H_2O or D_2O and relyophilized twice. The desired product was obtained in 82% yield as a flaky white powder: ^{1}H NMR (500 MHz, D_2O) δ 8.60 (s, 1H), 8.31 (s, 1H), 6.98−6.92 (dt, 1H, J = 15.5, 7.1 Hz), 6.19 (d, 1H), 6.17 (d, 1H, J = 15 Hz), 4.85 (t, 1H), 4.60 (s, 1H), 4.25 (s, 2H), 4.05 (s, 1H), 3.87 (q, 1H), 3.60 (q, 1H), 3.50 (t, 2H), 3.38 (t, 2H), 3.06 (t, 2H), 2.56 (t, 2H), 2.26 (t, 2H), 1.42 (m, 2H), 1.23 (bm, 12H), 0.92 (s, 3H), 0.83 (t, 3H), 0.78 (s, 3H); UV−vis (H_2O) ϵ_{260} 20.4 mM^{-1} cm^{-1}; MADLI-MS ($[M - H]^-$) calcd for $[C_{33}H_{53}N_7O_{17}S]^-$ 946.2, found 946.3.

Preparation of 4(S)-NADD. 4(*S*)-NADD was enzymatically synthesized essentially as described previously (*17*, *18*). One hundred milligrams (550 μmol) of [1-D]glucose, 33 mg (50 μmol) of β-NAD^+, and 40 units of glucose-6-phosphate dehydrogenase from *L. mesenteroides* (EC 1.1.1.49) were dissolved in 2 mL of 40% DMSO/100 mM sodium phosphate (pH 8) at 25 °C. The progress of the reaction was followed by monitoring the increase in absorbance at 340 nm and the A_{260}/A_{340} ratio. After 2 h at 25 °C, the reaction had gone to

Table 1: Primers Used for Mutagenesis[a]

mutant	primer[b]
Y158A (forward, F)	5′-CGGGCGATGCCGGCC**GCC**AACTGGATGACGGTC-3′
Y158A (reverse, R)	5′-GACCGTCATCCAGTT**GGC**GGCCGGCATCGCCCG-3′
Y158F (F)	5′-CGGGCGATGCCGGCC**TTC**AACTGGATGACGGTC-3′
Y158F (R)	5′-GACCGTCATCCAGTT**GAA**GGCCGGCATCGCCCG-3′
Y158S (F)	5′-CGGGCGATGCCGGCC**AGC**AACTGGATGACGGTC-3′
Y158S (R)	5′-GACCGTCATCCAGTT**GCT**GGCCGGCATCGCCCG-3′
K165A (F)	5′-GATGACGGTCGCC**GAC**AGCGCGTTGGAG-3′
K165A (R)	5′-CTCCAACGCGCT**GCG**GGCGACCGTCATC-3′
K165M (F)	5′-GATGACGGTCGCC**ATG**AGCGCGTTGGAG-3′
K165M (R)	5′-CTCCAACGCGCT**CAT**GGCGACCGTCATC-3′
K165Q (F)	5′-GATGACGGTCGCC**CAG**AGCGCGTTGGAG-3′
K165Q (R)	5′-CTCCAACGCGCT**CTG**GGCGACCGTCATC-3′
K165R (F)	5′-GATGACGGTCGCC**AGG**AGCGCGTTGGAG-3′
K165R (R)	5′-CTCCAACGCGCT**CCT**GGCGACCGTCATC-3′

[a] Forward and reverse primers are listed. [b] Mutation site is underlined in bold.

completion and the A_{260}/A_{340} ratio had reached 2.4. The reduced nucleotide was then purified by Pharmacia Biotech fast-protein liquid chromatography (FPLC) (*18*). The enzyme was removed by centrifugation with a centricon YM10 membrane (Amicon), and the 4(*S*)-NADD was isolated by FPLC using a Mono Q HR10/10 anion exchange column. Chromatography was performed using 10 mM triethanolamine (pH 7.8) as buffer A and running a 0 to 15% gradient of 10 mM triethanolamine and 1 M KCl (pH 7.8) (buffer B) over the course of 80 min at a flow rate of 4 mL/min. Elution was monitored at 254 nm. The reduced nucleotide eluted at 38 min, and fractions with an A_{260}/A_{340} ratio of ≤ 2.3 were pooled, concentrated in vacuo, and desalted on a Phenomenex C_{18} reverse phase HPLC column: ^{1}H NMR (500 MHz, D_2O) δ 8.50 (s, 1H), 8.25 (s, 1H), 6.98 (s, 1H), 6.14−6.12 (d, 1H, $J = 9.99$ Hz), 6.00−5.98 (d, 1H, $J = 9.99$ Hz), 4.81 (s, 1H), 4.78 (s, 1H), 4.71 (t, 1H), 4.51 (s, 1H), 4.39 (bm, 1H), 4.25 (m, 1H), 4.23 (m, 2H), 4.18 (m, 1H), 4.08 (bm, 3H), 2.78 (s, 1H); UV−vis (H_2O) $A_{260}/A_{340} = 2.27$; MADLI-MS ($[M - H]^-$) calcd for $[C_{21}H_{27}DN_7O_{14}P_2]^-$ 665.1, found 665.0.

Construction of Expression Plasmids for Wild-Type and Mutant InhAs. A pET15(b) expression plasmid containing the gene for wild-type InhA was a kind gift from J. Blanchard at the Albert Einstein College of Medicine (Bronx, NY) (*3*). To facilitate purification of the enzyme, the gene for InhA was subcloned out of this vector using PCR and inserted into a pET15(b) plasmid downstream of a His tag sequence. The PCR primers that were used were 5′-CTTTAAGAAGGAGATATCATATGACAGGACTGCTGGACGGC-3′ and 5′-GACGCCGGATCCTAGAGCATTTGG-3′, which introduced a 5′ *Nde*I restriction site and a 3′ *Bam*HI restriction site (underlined). Mutations were introduced using the QuikChange mutagenesis kit (Stratagene). A list of the primers that were used for mutagenesis is given in Table 1. Wild-type and mutant plasmids were purified from XL1Blue cells (Stratagene) using a DNA purification and gel extraction kit from Qiagen Inc., sequenced using dideoxynucleotide methodology with [^{35}S]dATP (Sequenase 2, U.S. Biochemicals or CircumVent Thermal Cycle Dideoxy DNA Sequencing Kit), and transformed into BL21(DE3)pLysS cells (Novagen) for protein expression.

Overexpression and Purification of Wild-Type and Mutant InhAs. Cultures of BL21(DE3)pLysS cells carrying the wild-type and mutant plasmids were grown in 500 mL of LB-ampicillin (300 μg/mL) medium at 37 °C to an OD_{600} of 1.6. The cells were harvested by centrifugation and resuspended in an equal volume of fresh LB-ampicillin containing isopropyl β-D-thiogalactoside (360 μg/mL). After an overnight induction at 25 °C, the cells were harvested by centrifugation, resuspended in 40 mL of His-bind buffer, and lysed using a French press (five passes at 1500 psi). Cell debris was removed by centrifugation (40 000 rpm for 60 min) and the supernatant applied to a His-bind resin column (5 mL bed volume). The His-bind column was washed successively with His-bind buffer and His-wash buffer, and the protein was eluted using a gradient of 0 to 1 M imidazole in 20 mM Tris-HCl and 500 mM NaCl (pH 7.9). Fractions containing His-tagged InhA were immediately pooled and applied to a 2 cm × 50 cm Sephadex G-25 column (Pharmacia) equilibrated with 20 mM Tris-HCl, 150 mM NaCl, and 2.5 mM $CaCl_2$ (pH 8.4). It is important that the eluted protein is not allowed to remain in the imidazole elute buffer as this causes the protein to precipitate. Fractions containing the His-tagged protein from the G-25 column were pooled, and the His tag was removed using biotinylated thrombin (1 unit/mg of protein). The cleavage reaction was monitored using SDS−PAGE and was shown to be complete after 24 h. Subsequently, the thrombin was removed using streptavidin−agarose (20 μL/unit of thrombin) and the protein exchanged into PIPES buffer (pH 6.8) containing 150 mM NaCl. The purified enzyme was stable for 3 months in 30 mM PIPES, 150 mM NaCl, and 1 mM EDTA at pH 6.8 and 4 °C. The concentration of the protein was calculated from the UV absorption at 280 nm using an absorption coefficient of 37.3 mM^{-1} cm^{-1} for the wild type and K165 mutants (*3*) and 35.7 mM^{-1} cm^{-1} for the Y158F and Y158A enzymes.

For the purposes of comparison, wild-type InhA was also expressed using the original pET15(b) expression plasmid and purified as described previously (*3*).

Circular Dichroism Spectroscopy. Circular dichroism (CD) spectroscopy was carried out using an AVIV model 62A DS spectrometer equipped with a Peltier temperature control unit. Far-UV CD spectra (250−190 nm) of wild-type and mutant proteins (12 μM) were acquired at 25 °C in 10 mM Na_2HPO_4 and 100 mM NaCl (pH 7.5).

NMR Spectroscopy. ^{1}H NMR spectra were obtained using a Varian Inova 500 and 600 MHz spectrometer. ^{1}H NMR spectra were processed on a Silicon Graphics Indigo2 workstation with the program FELIX (Molecular Simulations

Inc.). All NMR spectra were obtained at 25 °C using TSP-d_4 as an internal standard.

Fluorescence Titration Experiments. Equilibrium fluorescence titration was conducted using a model FL3-21 Fluorolog-3 spectrofluorometer (Edison, NJ). All measurements were carried out in 100 mM PIPES (pH 7) at 25 °C. The excitation wavelength was 360 nm (5 nm slit width), and the emission wavelength was 440 nm (1 nm slit width). Experiments were carried out as previously described (*7*). Briefly, in a typical experiment, 1 μL aliquots of 3 mM NADH were added to a 3 mL solution of 0.5−2 μM protein. The fluorescence intensity was recorded as an average of 60 readings (2 s). Dilution of protein was kept to a minimum (<1%). Data could not be fit to a simple hyperbolic function. Instead, data were fit to the following quadratic equation (eq 1):

$$\frac{F_e - F_l}{F_e(\max) - F_l(\max)} = \frac{(K_d + [E]_0 + [NADH]) - \sqrt{(K_d + [E]_0 + [NADH])^2 - 4K_d[E]_0}}{2[E]_0} \quad (1)$$

where F_e and F_l are the fluorescence intensity in the presence and absence of enzyme, respectively, F_e(max) and F_l(max) are the maximum fluorescence intensity in the presence and absence of enzyme, respectively, K_d is the dissociation constant, $[E]_0$ is the total enzyme concentration, and [NADH] is the concentration of added NADH. Data fitting was accomplished using the software program Grafit 3.09b (Erithacus Software Ltd.).

For the Y158A enzyme, NADH binding curves were not hyperbolic but sigmoidal. These data were fit to the Hill equation for cooperative binding (eq 2) for values of Y between 0.1 and 0.9.

$$\log[Y/(1 - Y)] = n \log[X] - \log K' \quad (2)$$

where $Y = (F_e - F_l)/[F_e(\max) - F_l(\max)]$, n is the Hill coefficient, [X] is $[NADH]_{free}$, and K' is a constant comprising the factor of interaction between the subunits and the intrinsic dissociation constant (*19*).

Steady State Kinetics. All experiments were carried out on a Cary 100 Bio (Varian) spectrophotometer at 25 °C in 30 mM PIPES and 150 mM NaCl (pH 6.8). Identical kinetic parameters were obtained when the concentration of PIPES was raised to 100 mM, indicating that there was no buffer effect on enzyme activity. Kinetic parameters were determined spectrophotometrically by following the oxidation of NADH to NAD^+ at 340 (ϵ = 6.3 mM^{-1} cm^{-1}) or 370 nm (ϵ = 2.4 mM^{-1} cm^{-1}). k_{cat} and k_{cat}/K_m for *trans*-2-dodecenoyl-CoA (DD-CoA) were determined at a fixed, saturating concentration of NADH (250 μM) and by varying the concentration of DD-CoA (0−200 μM). k_{cat} and k_{cat}/K_m for NADH were determined at a fixed concentration of DD-CoA (150 μM) and by varying the concentration of NADH (0−500 μM). Higher concentrations of DD-CoA could not be used as increasing the concentration above 150 μM resulted in a decrease in rate, possibly due to substrate inhibition (*7*). Each initial velocity was determined in triplicate, and at least five different substrate concentrations were examined. Kinetic parameters, k_{cat} and K_m, were obtained by fitting the initial velocity data to eq 3 using Grafit 3.09b (Erithacus Software Ltd.) where [S] is the concentration of the varied substrate.

$$v = k_{cat}[E]_0[S]/(K_m + [S]) \quad (3)$$

Alternatively, where both the NADH and DD-CoA concentrations were varied, k_{cat} and K_m values were obtained by fitting the data to eq 4 where K_{dA} is the K_d for substrate A, K_A is the K_m for substrate A, and K_B is the K_m for substrate B.

$$v = V_{max}[A][B]/(K_{dA} + K_A[B] + K_B[A] + [A][B]) \quad (4)$$

Solvent Kinetic Isotope Effect. Solvent deuterium kinetic isotope effects on V (^{D_2O}V) and V/K ($^{D_2O}V/K$) were determined at pH(D) 6.8 in 30 mM PIPES containing 150 mM NaCl. For reactions performed in D_2O, the buffer was titrated to pD 6.8 using DCl, where pD is equal to the pH meter reading plus 0.4 (*20*). Kinetic parameters were determined at a fixed, saturating concentration of NADH (250 μM) and by varying the concentration of DD-CoA (0−200 μM). Alternatively, the kinetic isotope effects were determined at a fixed concentration of DD-CoA (150 μM) and by varying the concentration of NADH (0−500 μM). Each initial velocity was determined in triplicate, and at least five different substrate concentrations were examined. Kinetic data were fit to the following equation (eq 5) using Grafit:

$$v = [S]/(\{1/[VK(1 + fi \times E_{V/K})]\} + [S]/[V(1 + fi \times E_V)]) \quad (5)$$

where [S] is the concentration of the varied substrate, VK = V/K, fi is the fraction of D in the reaction (0−1.0), and $E_{V/K}$ and E_V are the isotope effects minus one on V/K and V, respectively. Since V/K is evaluated as a single parameter, this enabled errors for V and V/K to be estimated accurately. k_{cat} and k_{cat}/K_m values for the wild-type enzyme were shown to be identical at pH 5.0 and 8.0, indicating that the pH used to determine the solvent isotope effects (6.8) was not close to an ionization affecting enzyme activity (*21*).

Multiple kinetic isotope effects on V ($^{D_2O}V_D$), V/K_{NADH} ($^{D_2O}V/K_{D\ NADH}$), and V/K_{DDCoA} ($^{D_2O}V/K_{D\ DDCoA}$) were determined by measuring the solvent isotope effect on V and V/K as described above except that NADH was replaced by *pro*-4(*S*) NADD.

Primary Kinetic Isotope Effects. Primary deuterium kinetic isotope effects on V (^DV) and V/K ($^DV/K$) were determined at a fixed, saturating concentration of NADH or 4(*S*)-NADD (250 μM) and by varying the concentration of DD-CoA (0−200 μM). Alternatively, the kinetic isotope effects were determined at a fixed concentration of DD-CoA (150 μM) and by varying the concentration of NADH or 4(*S*)-NADD (0−500 μM). In each case, the initial velocity data were fit to eq 5 using an fi of 0.98.

RESULTS

Expression, Purification, and Characterization of InhA Using an N-Terminal His Tag. To simplify the purification of InhA, the protein was expressed with an N-terminal His tag sequence. This enabled the single-step purification of protein using metal affinity chromatography. The method

Table 2: Kinetic Parameters for Wild-Type and Mutant InhA Enzymes[a]

enzyme	k_{cat} (min^{-1})	K_m (μM) DD-CoA	K_m (μM) NADH	k_{cat}/K_m (μM^{-1} min^{-1}) DD-CoA
wild-type[b]	278 ± 26	27 ± 7	ND[d]	10.3 ± 3.6
wild-type with His tag	434 ± 19	48 ± 7	65 ± 7	9.1 ± 1.7
wild-type[c]	501 ± 23	46 ± 5	66 ± 7	10.9 ± 1.7
Y158F[c]	21 ± 7	70 ± 6	2.0 ± 0.1	0.3 ± 0.1
Y158A[c]	0.33 ± 0.01	54 ± 6	5 ± 1	0.006 ± 0.001
Y158S[c]	410 ± 27	48 ± 8	48 ± 8	8.5 ± 2.0
K165Q[c]	680 ± 42	62 ± 10	66 ± 5	11.0 ± 0.2
K165R[c]	658 ± 36	54 ± 8	51 ± 5	12.1 ± 2.1

[a] Kinetic parameters were determined at 25 °C. [b] Enzyme prepared without the His tag. [c] Enzyme prepared with the His tag removed. [d] Not determined.

yielded approximately 75 mg of protein from 500 mL of bacterial culture. Even with heavy loading, no other bands could be detected on a SDS−PAGE gel. The His tag sequence contained a thrombin cleavage site, and biotinylated thrombin was used to remove the His tag. This procedure was monitored by SDS−PAGE as the His tag sequence added ca. 2 kDa to the apparent molecular mass of the protein. Following cleavage, the protein was exposed to streptavidin−Sepharose and His-bind resin to remove the biotinylated thrombin and uncleaved InhA as well as the His tag peptide. Following removal of the His tag, the InhA protein has four additional N-terminal amino acids (GSHM) compared to the mature protein.

Steady State Kinetic Analysis of Wild-Type Proteins. The k_{cat} and K_m values for wild-type InhA, purified with and without the His tag method, are given in Table 2. InhA purified using the original expression plasmid (*3*) exhibited a k_{cat} of 278 ± 26 min^{-1} and a $K_{m\,DDCoA}$ of 27 ± 7 μM. The corresponding values for InhA purified using the His tag method are 434 ± 19 min^{-1} (k_{cat}) and 48 ± 7 μM ($K_{m\,DDCoA}$), before removal of the His tag, and 501 ± 23 min^{-1} (k_{cat}) and 46 ± 5 μM ($K_{m\,DDCoA}$), after removal of the His tag. These values are within a factor of 2 of each other and are also within the range of values previously published for InhA [k_{cat} = 165 ± 14 min^{-1} and $K_{m\,DDCoA}$ = 48 ± 6 μM (*3*); k_{cat} = 941 ± 29 min^{-1} and $K_{m\,DDCoA}$ = 75 ± 5 μM (*7*)]. In addition, the $K_{m\,NADH}$ values determined for the His-tagged InhA before (65 ± 7 μM) and after (66 ± 7 μM) removal of the His tag were identical and similar to the previously reported value of 56 ± 4 μM (*7*). Although the His tag sequence did not alter the kinetic parameters of the enzyme, it reduced the solubility of the protein at pH 6.8, presumably due to an increase in the pI of the protein. Consequently, the His tag sequence was routinely removed by thrombin cleavage prior to kinetic analysis.

Steady State Kinetic Analysis of Mutant Proteins. Table 2 lists the k_{cat} and K_m values for the Y158F, Y158A, Y158S, K165Q, and K165R mutants of InhA. The Y158S, K165Q, and K165R proteins all had k_{cat}, $K_{m\,DDCoA}$, and $K_{m\,NADH}$ values similar to those of wild-type InhA. The Y158F and Y158A proteins had $K_{m\,DDCoA}$ values of 70 ± 6 and 54 ± 6 μM, respectively, similar to values for the wild-type InhA. However, the k_{cat} and $K_{m\,NADH}$ values were substantially reduced compared to those of the wild type with a k_{cat} of 21 ± 7 min^{-1} and a $K_{m\,NADH}$ of 2.0 ± 0.1 μM, for Y158F, and a k_{cat} of 0.33 ± 0.01 min^{-1} and a $K_{m\,NADH}$ of 5 ± 1 μM, for Y158A. Consequently, replacement of Y158 with F and A results in 24- and 1500-fold reductions in k_{cat}, respectively.

Table 3: K_d Values for NADH Binding to Wild-Type and Mutant InhA Enzymes[a]

enzyme	K_d (μM)	enzyme	K_d (μM)
wild-type	0.48 ± 0.03	K165Q	0.14 ± 0.02
Y158F	0.19 ± 0.01	K165R	0.09 ± 0.02
Y158S	0.06 ± 0.01		

[a] K_d determined by fluorescence titration. Enzyme concentrations were 1.86 (wild-type), 2.35 (Y158F), 1.20 (Y158S), 0.92 (K165Q), 2.13 (K165R), 2.10 (K165A), and 1.10 μM (K165M). All enzymes were expressed with the His tag sequence which was removed prior to determining the K_d values.

CD Spectra of Wild-Type and Mutant InhA Proteins. As evidence for correct folding of the mutant proteins, CD spectra of the wild type and two mutant proteins (Y158F and K165A) were obtained. All three had virtually superimposable CD spectra (data not shown), indicating that the decreased enzyme activity (Y158F) or lowered affinity for NADH (K165A) for these two mutants was not due to a major structural change in the protein. Using software supplied with the instrument, the α-helix contents for the wild-type, Y158F, and K165A enzymes were estimated to be 37, 36, and 38%, respectively.

Equilibrium Binding of NADH to Wild-Type and Mutant InhA Proteins. Dissociation constants (K_d) for the interaction of NADH with the wild-type and mutant InhA proteins were determined by fluorescence spectroscopy (*7*). For the wild-type, Y158F, Y158S, K165Q, and K165R proteins, NADH binding curves were hyperbolic and K_d values were calculated by fitting the data to eq 1. The values that were obtained were 0.48 ± 0.03 μM for the wild type, 0.19 ± 0.01 μM for Y158F, 0.06 ± 0.01 μM for Y158S, 0.14 ± 0.02 μM for K165Q, and 0.09 ± 0.02 μM for K165R (Table 3). The value for the wild-type protein was very similar to that reported previously [0.57 ± 0.04 (*7*)]. NADH binding to the Y158A enzyme was not hyperbolic but sigmoidal. Inspection of the binding curve indicated that NADH binding was 50% complete at 10 μM NADH. Fits of the data to the Hill equation (eq 2) gave a Hill coefficient of 2.1 ± 0.1 and a K' of (2.0 ± 0.1) × 10^{-11}. In addition, no detectable NADH binding was observed for the K165A and K165M mutants even up to 1 mM NADH, indicating a K_d of >1 mM for these enzymes.

Solvent Isotope Effects on Wild-Type and Mutant InhA Proteins. Solvent kinetic isotope effects are given in Tables 4 and 5. For the wild-type enzyme, a small normal kinetic solvent isotope effect of 1.51 ± 0.19 was observed on V (^{D_2O}V), while a larger normal effect was observed on V/K with NADH as the varied substrate ($^{D_2O}V/K_{NADH}$ = 2.46 ± 0.13). In contrast, an inverse kinetic isotope effect of 0.59 ± 0.18 was observed on V/K with DD-CoA as the varied substrate ($^{D_2O}V/K_{DDCoA}$).

Compared to that of the wild type, a small increase in ^{D_2O}V was observed for the Y158S mutant (2.05 ± 0.07), while $^{D_2O}V/K_{DDCoA}$ (0.47 ± 0.23) and $^{D_2O}V/K_{NADH}$ (2.30 ± 0.38) were similar to those of the wild type. The Y158F and Y158A mutants had smaller isotope effects on both V and V/K. For Y158A, ^{D_2O}V (1.27 ± 0.22), $^{D_2O}V/K_{DDCoA}$ (1.14 ± 0.23), and $^{D_2O}V/K_{NADH}$ (1.14 ± 0.21) were close to, or

Table 4: Kinetic Isotope Effects for Wild-Type and Y158 Mutant InhA Enzymes[a]

	H_2O[b]	D_2O[c]	SIE[d]
	Wild-Type		
V	3.33 ± 0.10	0.90 ± 0.11	1.51 ± 0.19
V/K_{NADH}	1.97 ± 0.23	1.06 ± 0.17	2.46 ± 0.13
V/K_{DDCoA}	2.36 ± 0.52	0.43 ± 0.10	0.59 ± 0.18
	Y158F		
V	2.50 ± 0.15	0.91 ± 0.13	1.39 ± 0.17
V/K_{NADH}	2.06 ± 0.19	0.93 ± 0.24	1.18 ± 0.24
V/K_{DDCoA}	2.36 ± 0.25	0.83 ± 0.26	0.73 ± 0.22
	Y158A		
V	2.40 ± 0.10	1.08 ± 0.09	1.27 ± 0.22
V/K_{NADH}	2.02 ± 0.60	0.87 ± 0.26	1.14 ± 0.23
V/K_{DDCoA}	2.49 ± 0.45	0.89 ± 0.17	1.14 ± 0.21
	Y158S		
V	3.50 ± 0.07	0.86 ± 0.18	2.05 ± 0.17
V/K_{NADH}	1.90 ± 0.33	0.88 ± 0.20	2.30 ± 0.38
V/K_{DDCoA}	2.38 ± 0.38	0.59 ± 0.16	0.47 ± 0.23

[a] Kinetic parameters were determined at 25 °C. All enzymes were purified using the His tag method and had the His tag sequence removed prior to kinetic analysis. [b] Isotope effect determined in H_2O using NADD. [c] Isotope effect determined in D_2O using NADD. [d] SIE is the solvent isotope effect.

Table 5: Kinetic Isotope Effects for Wild-Type and K165 Mutant InhA Enzymes[a]

	H_2O[b]	D_2O[c]	SIE[d]
	Wild-Type		
V	3.33 ± 0.10	0.90 ± 0.11	1.51 ± 0.19
V/K_{DDCoA}	2.36 ± 0.52	0.43 ± 0.10	0.59 ± 0.18
	K165Q		
V	2.42 ± 0.30	1.38 ± 0.31	1.53 ± 0.26
V/K_{DDCoA}	3.34 ± 0.37	0.7 ± 0.3	0.58 ± 0.25
	K165R		
V	2.34 ± 0.26	1.34 ± 0.24	1.59 ± 0.21
V/K_{DDCoA}	3.68 ± 0.32	0.7 ± 0.3	0.74 ± 0.50

[a] Kinetic parameters were determined at 25 °C. All enzymes were purified using the His tag method and had the His tag sequence removed prior to kinetic analysis. [b] Isotope effect determined in H_2O using NADD. [c] Isotope effect determined in D_2O using NADD. [d] SIE is the solvent isotope effect.

indistinguishable from, unity (Table 4). For Y158F, the ^{D_2O}V (1.39 ± 0.17) was intermediate between the values observed for the wild type and Y158A enzymes. In addition, $^{D_2O}V/K_{DDCoA}$ (0.73 ± 0.22) and $^{D_2O}V/K_{NADH}$ (1.18 ± 0.24) were close to unity.

^{D_2O}V values for the K165Q (1.53 ± 0.26) and K165R (1.59 ± 0.21) enzymes as well as $^{D_2O}V/K_{DDCoA}$ for K165Q (0.58 ± 0.25) were also very similar to that of wild-type InhA. $^{D_2O}V/K_{DDCoA}$ for K165R (0.74 ± 0.50) was indistinguishable from unity.

Primary Kinetic Deuterium Isotope Effects on Wild-Type and Mutant InhA Proteins. Primary kinetic deuterium isotope effects resulting from the use of 4(*S*)-NADD are reported in Tables 4 and 5. For the wild-type enzyme, ^{D}V and $^{D}V/K_{DDCoA}$ were 3.33 ± 0.10 and 2.36 ± 0.52, respectively, similar to previously reported values (*3*). With NADH(D) as the variable substrate, the isotope effect on V/K ($^{D}V/K_{NADH}$) was 1.97 ± 0.23, which is the same, within experimental data, as $^{D}V/K_{DDCoA}$. The similarity in $^{D}V/K$ values is consistent with the random order of addition of substrates to the enzyme, which varies slightly from data published by Blanchard and co-workers where it was concluded that the addition of substrates to the enzyme was not strictly ordered, but that the initial binding of NADH was preferred (*3*).

For the Y158S mutant, primary isotope effects on ^{D}V (3.50 ± 0.07), $^{D}V/K_{NADH}$ (1.90 ± 0.33), and $^{D}V/K_{DDCoA}$ (2.38 ± 0.38) were similar to those observed for the wild-type enzyme. For the Y158F and Y158A mutants, the ^{D}V values of 2.50 ± 0.15 and 2.40 ± 0.10 were slightly smaller than that for the wild-type enzyme. $^{D}V/K_{DDCoA}$ and $^{D}V/K_{NADH}$ values for Y158F and Y158A were, within error, the same as for the wild-type enzyme.

For the K165Q and K165R enzymes, primary isotope effects were only obtained by varying the concentration of DD-CoA. This gave a ^{D}V of 2.42 ± 0.30 and a $^{D}V/K_{DDCoA}$ of 3.34 ± 0.37 for K165Q and a ^{D}V of 2.34 ± 0.26 and a $^{D}V/K_{DDCoA}$ of 3.68 ± 0.32 for K165R. Thus, ^{D}V values for K165Q and K165R were similar to the values observed for the Y158 mutants but smaller than that for the wild-type enzyme, while $^{D}V/K_{DDCoA}$ values were similar to that of the wild-type enzyme.

Multiple Kinetic Isotope Effects on Wild-Type and Mutant InhA Proteins. Multiple kinetic isotope effects were determined by measuring the solvent isotope effect in the presence of 4(*S*)-NADD (Tables 4 and 5). In every instance, the solvent isotope effect on V ($^{D_2O}V_D$) was, within experimental error, indistinguishable from unity, consistent with a stepwise mechanism. For the wild type and Y158 mutants, the multiple isotope effects on V/K caused by varying the NADD concentration ($^{D_2O}V/K_{D\ NADD}$) were indistinguishable from unity. Importantly, however, for the wild type and Y158S, varying the DD-CoA concentration gave inverse isotope effects on $^{D_2O}V/K_{D\ DDCoA}$ of 0.43 ± 0.10 and 0.59 ± 0.16, respectively. In contrast, for Y158F and Y158A, the $^{D_2O}V/K_{D\ DDCoA}$ values were indistinguishable from unity.

DISCUSSION

Mechanism of Wild-Type InhA. Previous studies with InhA have resulted in the proposal that substrate reduction occurs via a stepwise mechanism in which hydride transfer precedes protonation (*3*). The results presented here are consistent with a stepwise mechanism in which the transition states for hydride transfer and protonation of the enol(ate) intermediate are both partially rate-limiting. This is based on the normal primary isotope effect on V using NADD ($^{D}V = 3.33 \pm 0.10$) and the small but normal solvent isotope effect on V ($^{D_2O}V = 1.51 \pm 0.19$). A multiple-isotope effect experiment confirms this conclusion; the solvent isotope effect on V using NADD as the substrate yields a $^{D_2O}V_D$ of 0.90 ± 0.11. The observation that the solvent isotope effect is smaller with NADD than with NADH is conclusive evidence that the primary and solvent isotope effects affect different steps in the mechanism. Thus, replacement of NADH by NADD affects the rate of hydride transfer, leading to the formation of the enol(ate) intermediate, while the solvent isotope sensitive step is assumed to be the breakdown of the enol(ate) intermediate by protonation at C2.

The observation that $^{D}V/K_{DDCoA}$ (2.36 ± 0.52) and $^{D}V/K_{NADH}$ (1.97 ± 0.23) are the same within experimental error is consistent with a mechanism in which substrates bind to the enzyme in a random order. If the mechanism were strictly ordered with NADH binding first, then a $^{D}V/K_{NADH}$ of unity

Scheme 2

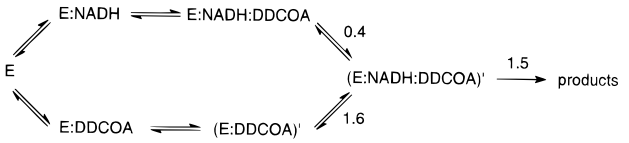

Scheme 3

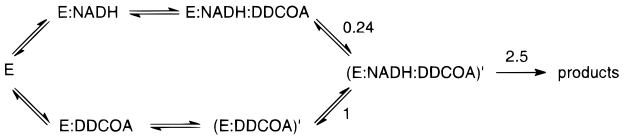

would be expected (*22*). Previously, Blanchard and co-workers reported a $^{D}V/K_{NADH}$ of greater than unity but smaller than $^{D}V/K_{DDCoA}$, suggesting that the mechanism is not strictly ordered, but that the initial binding of the cofactor is preferred (*3*). While we are not able to explicitly explain this discrepancy, it is noteworthy that the concentration of DD-CoA used in the determination of $^{D}V/K_{NADH}$ may not be saturating (see Experimental Procedures).

When DD-CoA is used as the variable substrate, an inverse solvent isotope effect is observed on V/K ($^{D_2O}V/K_{DDCoA} = 0.59 \pm 0.18$). In contrast, when NADH is used as the variable substrate, a normal solvent isotope effect is observed on V/K ($^{D_2O}V/K_{NADH} = 2.46 \pm 0.13$), which is larger than the observed ^{D_2O}V (1.51 ± 0.19). One explanation for the inverse $^{D_2O}V/K_{DDCoA}$ involves an inverse equilibrium isotope effect of 0.4 on a conformational change that occurs at the same time as, or after, DD-CoA binding to the enzyme. Thus, since ^{D_2O}V is 1.51, $^{D_2O}V/K_{DDCoA}$ will be 1.51×0.4 (0.6). In addition, to account for the $^{D_2O}V/K_{NADH}$ of 2.46, there must then be a normal isotope effect of 1.6 for the binding of NADH to the E−DD-CoA complex. These isotope effects are summarized in Scheme 2 where the active conformation of the enzyme is given by (E:DDCOA)′ and (E:NADH:DDCOA)′. Alternatively, the intrinsic ^{D_2O}V may be the same as $^{D_2O}V/K_{NADH}$ (2.5), and the reduction in the observed ^{D_2O}V could result from the release of the second product being partially rate-limiting. Then, no equilibrium isotope effect would be required for NADH binding, but a larger inverse equilibrium isotope effect (0.24) would be required to account for the observed $^{D_2O}V/K_{DDCoA}$ of 0.59 ± 0.18. These isotope effects are summarized in Scheme 3 where the active conformation of the enzyme is given by (E:DDCOA)′ and (E:NADH:DDCOA)′. Replacement of NADH with 4(*S*)-NADD results in a solvent isotope effect on V that is indistinguishable from unity. This is consistent with a stepwise mechanism in which hydride transfer is now completely rate-limiting (see above). In contrast, the equilibrium isotope effects invoked to account for the solvent isotope effects on V/K should still be present when using 4(*S*)-NADD. The $^{D_2O}V/K_{D\ NADH}$ of 1.06 ± 0.17 is well-defined and indistinguishable from unity. This supports the model shown in Scheme 3 in which the observed $^{D_2O}V/K_{NADH}$ of 2.46 ± 0.13 is the intrinsic isotope effect (see above). However, we would still expect to observe an inverse isotope effect on V/K when varying the DD-CoA concentration in the presence of NADD. This is indeed what is observed. $^{D_2O}V/K_{D\ DDCoA}$ is 0.43 ± 0.10, which is consistent with an inverse equilibrium isotope effect following the binding of DD-CoA to the enzyme. Since the solvent isotope effect on V is now masked, the apparent $^{D_2O}V/K_{D\ DDCoA}$ should be more inverse than the solvent isotope effect using NADH ($^{D_2O}V/K_{DDCoA}$). Indeed, although the $^{D_2O}V/K_{D\ DDCoA}$ of 0.43 is nominally smaller than the $^{D_2O}V/K_{DDCoA}$ of 0.59, the errors in these two values prevent us from distinguishing between them. Nevertheless, the fact that an inverse solvent isotope effect on V/K_{DDCoA} is still observed when NADD is substituted for NADH is very significant.

We believe the structural basis for the conformational change proposed above represents rotation of Y158 into a position where it can hydrogen bond to the substrate carbonyl. This hypothesis is supported by the mutagenesis experiments with Y158, discussed below, and by the X-ray crystal structures determined by Sacchettini and co-workers (*1*, *15*). Comparison of the structure of the InhA−NADH binary complex with that of an inactive ternary complex formed by InhA, NAD^+, and a C16 enoyl substrate reveals that upon binding the enoyl substrate there is a 60° rotation about the Y158 $C_\alpha-C_\beta$ bond that enables Y158 to hydrogen bond to the substrate carbonyl group. The repositioning of Y158 is shown diagrammatically in Figure 1.

Mutagenesis of Y158, and NADH Binding. The Y158F enzyme has a K_d for NADH similar to that of the wild-type enzyme. In the Y158A enzyme, however, NADH binding is sigmoidal not hyperbolic. Sigmoidal binding curves are also observed for InhA mutants in which residues close to the NADH binding pocket have been altered (*7*). This has previously been attributed to cooperative NADH binding (*7*), which is possible since the active protein is a tetramer of identical subunits (*1*). The latter mutations result in substantial decreases in the affinity for NADH and increases in the K_m for NADH. However, both Y158F and Y158A have significantly *lower* K_m values for NADH compared to that of the wild type. The observation of cooperative binding of NADH to the Y158A mutant does not detract from the primary conclusion that Y158 is a key catalytic residue in the enzyme (see below).

Y158S. Given the conservation of Y158 throughout the enoyl reductase family (Table 6), it is remarkable that replacement of Y158 with serine results in an enzyme with properties virtually identical to those of the wild-type enzyme. Clearly, the serine hydroxyl group can fulfill the same function as the tyrosine hydroxyl group. Although the pK_a values of the tyrosine hydroxyl group in the wild-type enzyme and of the serine hydroxyl group in the Y158S enzyme are unknown, the pK_a values of these groups in the free amino acids are 10.5 and 15, respectively. Thus, it is unlikely that the role of the Y158 residue in the wild-type enzyme depends directly on the acidity of the hydroxyl group. This observation again mitigates against the possibility that the hydroxyl group of Y158 is a proton donor in the reaction. However, both the tyrosine and serine hydroxyl groups can function as hydrogen bond donors or acceptors. Taken together, the most probable role for Y158 is that it provides electrophilic stabilization of the transition state(s) for the reaction by hydrogen bonding to the carbonyl of the substrate. This function is analogous to that performed by the catalytic tyrosine in ketosteroid isomerase (*23*, *24*). Support for the role of Y158 as an electrophilic catalyst is provided by the crystal structure determined by Sacchettini and co-workers that shows Y158 hydrogen bonded to the substrate carbonyl. Since the serine side chain is shorter than

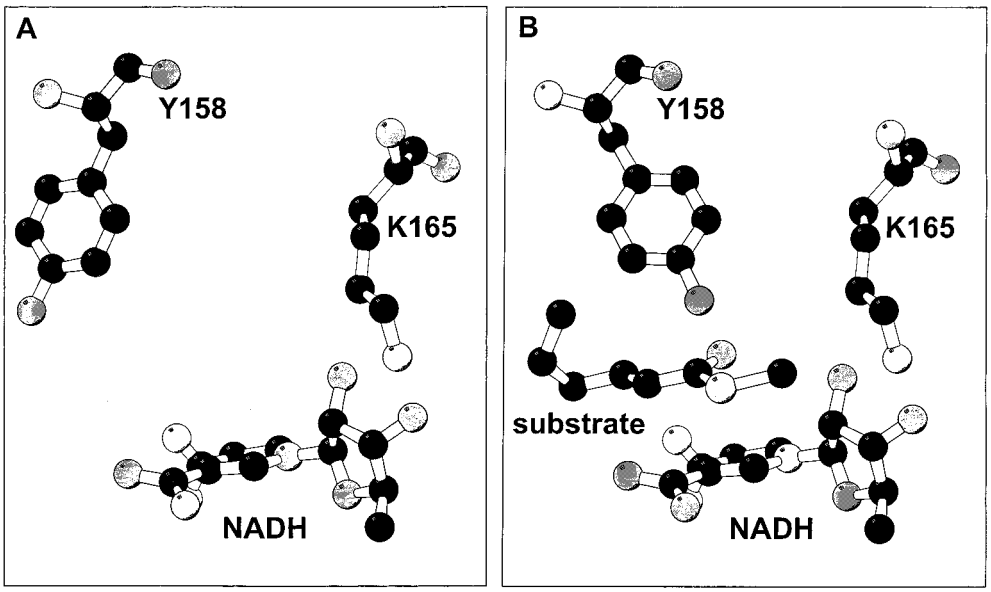

FIGURE 1: Model for the interaction of a simple substrate, *trans*-2-hexenoyl methyl thioester, with InhA, following rotation of Y158. The models are based on the X-ray structure of the InhA−NADH binary complex determined by Sacchettini and co-workers (*15*). The figure was generated using the program MOLSCRIPT (*70*). The atom colors are as follows: carbon, black; oxygen, dark gray; nitrogen and sulfur, light gray; and hydrogen, white. (A) Y158 oriented as in the X-ray structure of the InhA−NADH binary complex. (B) Y158 has been rotated by −60° about the $C_\alpha-C_\beta$ bond. The substrate is modeled in an s-cis conformation about the $C_3{=}C_2-C(=O)$ and is positioned so that the carbonyl group is within hydrogen bonding distance of the tyrosine hydroxyl. In addition, the C3 atom of the substrate is positioned 2 Å from the *pro*-4(*S*) NADH proton.

tyrosine, in the Y158S enzyme there must be a small structural change that enables the serine to interact directly with the substrate carbonyl, or a bridging water molecule is present between the serine hydroxyl and the substrate carbonyl group. Currently, there is no way to distinguish between these possibilities.

The isotope effects for Y158S are similar to those for the wild type. Significantly, using NADH or NADD, the solvent isotope effect on *V*/*K* with DD-CoA as the variable substrate is inverse. In contrast, for Y158F and Y158A, the solvent isotope effects on V/K_{DDCoA} are close to, or indistinguishable from, unity. Clearly, the presence of a hydroxyl group with a solvent exchangeable proton is critical for expression of the inverse isotope effect. This could result from changes in hydrogen bonding involving the side chain hydroxyl group that occur in the two conformations of the enzyme. To result in an inverse equilibrium isotope effect, the active conformation of the enzyme, in which Y158 is hydrogen bonded to the substrate, would have to be preferentially stabilized in D_2O as opposed to H_2O.

Y158F and Y158A. Replacement of Y158 with F and A results in a 24- and 1500-fold reduction in k_{cat}, respectively, while the K_m for DD-CoA is unaffected. Clearly, tyrosine 158 plays an important role in the chemical step(s) of substrate reduction. Additionally, the decrease in activity on replacing Y158 with F and with A correlates with a decrease in the magnitude of the solvent isotope effect on *V* with a ^{D_2O}V of 1.39 ± 0.17 for Y158F and 1.27 ± 0.22 for Y158A. Thus, the overall decrease in activity does not result from destabilization of the solvent isotope-sensitive transition state which is presumably protonation of the enol(ate) intermediate. This observation makes it unlikely that Y158 is the source of the proton required for the breakdown of the enol(ate) intermediate.

Since replacement of Y158 with F and A leads to a decrease in the magnitude of the solvent isotope effect, it might be expected that the isotope effect on hydride transfer would be larger. However, this is not observed. The ^{D}V values for the mutants are slightly smaller than for the wild type (2.5 vs 3.5). Thus, if mutagenesis of Y158 decreases the solvent isotope effect by raising the barrier for hydride transfer, the position of the transition state for hydride transfer must also be affected by the mutagenesis.

Replacement of Y158 with F and A also results in a decrease in the magnitude of the solvent isotope effects on *V*/*K*. For Y158A, both $^{D_2O}V/K_{NADH}$ and $^{D_2O}V/K_{DDCoA}$ are, within experimental error, unity. This indicates that the inverse equilibrium isotope effect, invoked to account for the inverse $^{D_2O}V/K_{DDCoA}$ in the wild-type enzyme, has been reduced in magnitude upon replacing the Y158 side chain with a methyl group. This result strengthens the assignment of the equilibrium isotope effect to a conformational change involving rotation of the Y158 side chain. Repositioning of the alanine side chain in Y158A upon binding DD-CoA represents a much smaller structural perturbation than movement of the tyrosine side chain.

The observation that $^{D_2O}V/K_{DDCoA}$ for Y158F is essentially unity indicates that the tyrosine hydroxyl is important for expression of the inverse equilibrium isotope effect associated with repositioning of the tyrosine side chain. This conclusion is supported by the close similarity in isotope effects between the wild-type enzyme and Y158S. The serine side chain is less bulky than tyrosine, but still possesses a side chain that can participate in hydrogen bonding. Finally, the fact that Y158F is more active than the Y158A enzyme could result from the phenyl group assisting in the positioning of a water molecule that fulfills part of the function of the tyrosine hydroxyl group.

Mutagenesis of K165. Replacement of K165 with A or M results in an enzyme that is unable to bind NADH. No activity could be observed even at high NADH concentrations (5 mM), and NADH concentrations of 1 mM failed to

Table 6: Alignment of Enoyl-Reductase and Short Chain Alcohol Dehydrogenase Enzymes[a]

enoyl-reductase enzyme	accession number														
M. tuberculosis InhA (*41*)	CAB02034	156	P	A	**Y**	N		W	M	T	V	A	**K**	S	A
Mycobacterium smegmatis InhA (*2*)	AAC43211	156	P	A	**Y**	N		W	M	T	V	A	**K**	S	A
Mycobacterium bovis InhA (*2*)	AAB60183	156	P	A	**Y**	N		W	M	T	V	A	**K**	S	A
Mycobacterium avium InhA (*42*)	AAC46204	155	P	A	**Y**	N		W	M	T	V	A	**K**	S	A
E. coli EnvM (*28*)	AAA17755	154	P	N	**Y**	N		V	M	G	L	A	**K**	A	S
Salmonella typhimurium EnvM (*29*)	AAA27059	154	P	N	**Y**	N		V	M	G	L	A	**K**	A	S
Haemophilus influenzae EnvM (*27*)	AAC23379	187	P	N	**Y**	N		V	M	C	L	A	**K**	A	S
Pseudomonas aeruginosa EnvM (*43*)	AAC95362	157	P	N	**Y**	N		V	M	G	M	A	**K**	A	S
Bacillus subtilis putative EnvM (*44*)	CAB13029	167	P	N	**Y**	N		V	M	G	V	A	**K**	A	S
Anabaena sp. sequence-specific DNA binding protein bifA gene (*45*)	AAD04184	162	P	N	**Y**	N		V	M	G	V	A	**K**	A	G
Pasteurella haemolytica putative EnvM (*46*)	AAB87478	127	P	N	**Y**	N		V	M	C	L	A	Q	S	L
Rickettsia prowazekii strain Madrid E putative EnvM (*47*)	CAA14824	155	P	N	**Y**	N		I	M	G	V	A	**K**	A	A
Helicobacter pylori putative EnvM (*48*)	AAD07262	153	A	H	**Y**	N		V	M	G	L	A	**K**	A	A
Brassica napus (oilseed rape) EnvM (*30*)	AAB20114	269	P	G	**Y**	G	G	G	M	S	S	A	**K**	A	A
Oryza sativa (rice) EnvM (*49*)	CAA05816	262	P	G	**Y**	G	G	G	M	S	S	A	**K**	A	A
Chlamydia trachomatis putative EnvM (*50*)	AAC67695	186	P	G	**Y**	G	G	G	M	N	A	A	**K**	A	A
Streptomyces collinus 1-cyclohexenylcarbonyl CoA reductase chcA (*51*)	AAC44655	156	P	T	**Y**	A		M	L	G	G	M	**K**	A	A
Streptomyces argillaceus EnvM for mithramycin biosynthesis (*52*)	CAA61992	155	P	R	**Y**	A		G	A	G	M	A	**K**	A	A

short chain alcohol dehydrogenases	accession number														
H. pylori putative 7-α-hydroxysteroid dehydrogenase (*48*)	AAD08058	161	P	N	**Y**	A		G	H	G	N	S	**K**	N	A
E. coli 7-α-hydroxysteroid dehydrogenase (*53*)	BAA01384	154	I	N	M	T		S	**Y**	A	S	S	**K**	A	A
M. tuberculosis putative 7-α-hydroxysteroid dehydrogenase (*41*)	CAB08708	191	R	W	F	G		A	**Y**	G	V	T	**K**	S	A
Streptomyces exfoliatus 20-β-hydroxysteroid dehydrogenase (*54*)	P19992	147	A	L	T	S		S	**Y**	G	A	S	**K**	W	G
human 11-β-hydroxysteroid dehydrogenase type 2 (*55*)	S62789	227	P	C	L	G		A	**Y**	G	T	S	**K**	A	A
human 11-β-hydroxysteroid dehydrogenase (*56*)	DXHUBH	178	P	M	V	A		A	**Y**	S	A	S	**K**	F	A
mouse 11-β-hydroxysteroid dehydrogenase (*57*)	P50172	178	P	M	I	A		P	**Y**	S	A	S	**K**	F	A
Comamonas testosteroni 3- or 17-β-hydroxysteroid dehydrogenase (*58*)	S62216	145	E	Q	Y	A		G	**Y**	S	A	S	**K**	A	A
Sus scrofa 17-β-estradiol dehydrogenase (*59*)	CAA55037	159	F	G	Q	A		N	**Y**	S	A	A	**K**	L	G
human 17-β-hydroxysteroid dehydrogenase (*60*)	P51659	159	F	G	Q	A		N	**Y**	S	A	A	**K**	L	G
human 17-β-20-α-hydroxysteroid dehydrogenase type 2 (*61*)	P37059	227	E	R	L	A		S	**Y**	G	S	S	**K**	A	A
Rattus norvegicus 15-hydroxyprostaglandin dehydrogenase (*62*)	AAB53027	146	T	Q	Q	P		V	**Y**	C	A	S	**K**	H	G
Ba. subtilis short chain alcohol dehydrogenase homologue (*44*)	CAB12226	186	P	T	L	I		D	**Y**	T	A	T	**K**	G	A
M. tuberculosis short chain alcohol dehydrogenase homologue (*41*)	CAB05057	150	P	G	T	A		A	**Y**	G	A	A	**K**	A	G
Actinomadura hibisca putative polyketide synthase (*63*)	BAA23150	151	S	Q	R	T		H	**Y**	T	A	A	**K**	A	G
mouse carbonyl reductase (*64*)	BAA05120	144	P	N	L	I		T	**Y**	S	S	T	**K**	G	A
Streptomyces paucimobilis 2,5-dichloro-2,5-cyclohexadiene-1,4-diol dehydrogenase (*65*)	BAA03444	149	P	M	H	G		E	**Y**	V	G	A	**K**	H	A
M. smegmatis 3-ketoacyl reductase fabG gene (*66*)	AAC69638	156	G	N	Q	A		N	**Y**	A	A	A	**K**	A	G
M. tuberculosis 3-ketoacyl reductase fabG gene (*66*)	AAC69639	148	G	N	Q	A		N	**Y**	A	A	S	**K**	A	G
E. coli UDP galactose-4-epimerase (*67*)	AAC73846	144	T	P	Q	S		P	**Y**	G	K	S	**K**	L	M
rat dihydropteridine reductase (*68*)	P11348	142	P	G	M	I		G	**Y**	G	M	A	**K**	G	A
Trypanosoma cruzi pteridine reductase (*69*)	AAC38850	177	P	G	F	C		V	**Y**	T	M	A	**K**	H	A
human mitochondrial 2,4-dienoyl-CoA reductase (*40*)	AAA67551	205	G	F	V	V		P	S	A	S	A	**K**	A	G

[a] References for the sequence information are given after each enzyme name. Accession numbers refer to the NCBI protein database. The conserved tyrosine and lysine residues are bold.

elicit an increase in fluorescence compared to that observed for free NADH. Consequently, the K_d for NADH in these two mutants must be >1 mM. The inability of these enzymes to bind NADH indicates that K165 plays a primary role in binding the cofactor. These observations are supported by the X-ray crystal structure of NADH bound to InhA in which the amino group of K165 is hydrogen bonded to the two ribose hydroxyl groups of NADH (*15*).

In contrast, both the K165Q and K165R mutants exhibit unimpaired affinities for NADH compared to that of the wild-type enzyme. Clearly, the glutamine and arginine side chains are able to effectively substitute for the NADH binding function of the lysine side chain. In addition, both the K165Q and K165R enzymes exhibit catalytic parameters similar to those of the wild-type enzyme. Thus, k_{cat}, $K_{m\ NADH}$, and $K_{m\ DDCoA}$ values for the K165Q and K165R enzymes are virtually identical to wild-type values. Kinetic isotope effects for K165Q and K165R are also close to wild-type values. Consequently, if, as has previously been suggested, K165 is functioning as an electrophile in the reaction (*3*), then the glutamine and arginine side chains are equally effective at providing electrophilic stabilization in the reaction. Although there is precedence for glutamine residues acting as electrophiles in enzyme-catalyzed reactions (*25*), the data here do not support a role for K165 over and above cofactor binding. In the X-ray structure of the substrate bound to InhA, K165 is not close to the substrate carbonyl, supporting the conclusion that K165 is primarily involved in binding NADH (*1*). Finally, it is interesting to note that the putative EnvM from *Pasteurella haemolytica* has a glutamine in place of the conserved lysine (Table 6).

Comparison of the Role of Y158 and K165 with the Role of Those from Homologous Enzymes. Sequence alignment demonstrates that Y158 and K165 in InhA are conserved residues in the enoyl-reductase family that also includes enoyl-reductases from other mycobacteria (*Mycobacterium smegmatis, Mycobacterium avium*, and *Mycobacterium bovis*) (*2*, *26*) and other bacteria (*E. coli*, *Salmonella typhimu-*

rium, and *Haemophilus influenzae*) (*27*−*29*) and enoyl-reductases from plants (*Brassica napus*) (*30*) (Table 6). X-ray crystallographic analysis has shown that Y158 and K165 in InhA are also structurally homologous with the conserved tyrosine and lysine residues in the enoyl-reductases (EnvM) from *E. coli* and *B. napus* except that in the InhA structure the tyrosine is rotated 86° about the $C_\alpha-C_\beta$ single bond relative to its position in EnvM. The structure of a diazaborine inhibitor bound to the *E. coli* enoyl-reductase demonstrates that both the tyrosine and lysine side chains interact with a hydroxyl group in the inhibitor, which is presumed to occupy a position similar to that of the substrate carbonyl oxygen. The structure of the antibacterial compound triclosan bound to EnvM also exhibits a key hydrogen bonding contact between the hydroxyl group of the inhibitor and the catalytic tyrosine (*71*). In addition, in the InhA structure determined with only NADH bound, it is impossible for both Y158 and K165 to hydrogen bond to the substrate carbonyl unless the tyrosine were to rotate upon substrate binding (*15*). The data presented here, together with the X-ray structure of a substrate bound to InhA (*1*), demonstrate that Y158 in InhA does rotate upon substrate binding, into a position similar to that occupied by the conserved tyrosine in EnvM.

The enoyl-reductases are also structurally homologous to the short chain alcohol dehydrogenase (SCAD) family. The SCAD enzymes have conserved tyrosine and lysine residues organized in a characteristic YxxxK motif, whereas in the enoyl-reductases, the tyrosine and lysine are separated by six or seven residues (*14*, *31*, *32*) (Table 6). X-ray crystal structures of several SCAD enzymes, including 3-α,20-*β*-hydroxysteroid dehydrogenase (*33*), 17-*β*(estrogenic)hydroxysteroid dehydrogenase (*34*), UDP-galactose-4-epimerase (*35*), and dihydropteridine reductase (*36*), demonstrate the structural homology of the conserved tyrosine and lysine residues. Furthermore, the catalytic importance of the tyrosine and lysine residues, together with a conserved serine residue, has been shown in several members of the SCAD family by site-directed mutagenesis [reviewed by Jörnvall et al. (*37*); see also Nakajin et al. (*38*)]. Detailed crystallographic and kinetic analysis of wild-type and site-directed mutants of UDP-galactose-4-epimerase revealed that the catalytic tyrosine in this enzyme (Y149), with assistance from the conserved serine (S124) residue, functions as a general acid and base to reversibly protonate and deprotonate, respectively, the ketone oxygen of the substrate. Superposition of the X-ray structures of members of the SCAD family with the structures of the enoyl-reductase family indicates that both tyrosine and lysine side chains occupy very similar positions in all the enzymes.

Finally, there is also structural homology between the SCAD family and the aldo-keto reductase (AKR) enzymes, of which 3-α-hydroxysteroid dehydrogenase (3αHSD) is the best characterized member. Four catalytic residues have been identified in 3αHSD, Y55, K84, D50, and H117. While there is no sequence homology between the AKR and SCAD families, analysis of the X-ray crystal structures reveals that Y55, K84, and H117 in 3αHSD (*39*) are structurally homologous to the tyrosine, lysine, and serine residues in the SCAD enzymes. Although 3αHSD catalyzes the transfer of the *pro*-4(*R*) NADH proton while the SCAD enzymes and the enoyl reductases are *pro*-4(*S*) specific, the nicotinamide headgroups in 3αHSD and the SCAD enzymes can be superimposed so that the transferred protons are oriented in the same direction. If this is done, then the catalytic tyrosine and lysine residues in the two classes of enzymes occupy similar positions, and H117 in 3αHSD occupies a position similar to that of the conserved serine in the SCAD family. Finally, K84 in 3αHSD does not hydrogen bond to the cofactor ribose but instead forms a salt bridge with D50. Results from mutagenesis and kinetic experiments have resulted in the proposal that Y55 in 3αHSD functions as a general acid and base to catalyze the reversible reduction of the dihydrotestosterone 3-α-keto group to a hydroxyl group.

Both the SCAD and AKR enzymes catalyze the reversible oxidation and reduction of substrates with tyrosine acting as the proton donor and acceptor, respectively, coupled with hydride transfer to and from the carbonyl carbon. In contrast, the enoyl-reductases only catalyze substrate reduction and the site of protonation is the C2 of the substrate and not a keto carbonyl oxygen. On the basis of the kinetic analysis of InhA mutants, we propose that Y158 in InhA provides catalytic assistance by hydrogen bonding to the carbonyl of the substrate. Given that the Y158S mutant has wild-type activity, it is unlikely that Y158 provides electrophilic catalysis by formally protonating the oxygen of the enolate intermediate, or that Y158 protonates the intermediate at the C2 position. Interestingly, sequence alignment shows that mammalian dienoyl-CoA reductase has a serine in place of a tyrosine in the YxxxK motif (*40*). The latter enzyme also catalyzes reduction of a C═C double bond rather than a carbonyl group.

ACKNOWLEDGMENT

We thank Professor John Blanchard for the gift of the InhA expression plasmid. We thank Dr. Adrian Whitty, Professor Phil Huskey, and Professor Vern Anderson for helpful discussions.

REFERENCES

1. Rozwarski, D. A., Vilcheze, C., Sugantino, M., Bittman, R., and Sacchettini, J. C. (1999) *J. Biol. Chem. 274*, 15582−15589.
2. Banerjee, A., Dubnau, E., Quemard, A., Balasubramanian, V., Um, K. S., Wilson, T., Collins, D., de Lisle, G., and Jacobs, W. R., Jr. (1994) *Science 263*, 227−230.
3. Quemard, A., Sacchettini, J. C., Dessen, A., Vilcheze, C., Bittman, R., Jacobs, W. R., Jr., and Blanchard, J. S. (1995) *Biochemistry 34*, 8235−8241.
4. Johnsson, K., King, D. S., and Schultz, P. G. (1995) *J. Am. Chem. Soc. 117*, 5009−5010.
5. Basso, L. A., Zheng, R. J., and Blanchard, J. S. (1996) *J. Am. Chem. Soc. 118*, 11301−11302.
6. Rozwarski, D. A., Grant, G. A., Barton, D. H. R., Jacobs, W. R., Jr., and Sacchettini, J. C. (1998) *Science 279*, 98−102.
7. Basso, L. A., Zheng, R., Musser, J. M., Jacobs, W. R., Jr., and Blanchard, J. S. (1998) *J. Infect. Dis. 178*, 769−775.
8. Kochi, A. (1991) *Tubercle 72*, 1−6.
9. Bloom, B. R., and Murray, C. J. (1992) *Science 257*, 1055−1064.
10. Perlman, D. C., El Sadr, W. M., Heifets, L. B., Nelson, E. T., Matts, J. P., Chirgwin, K., Salomon, N., Telzak, E. E., Klein, O., Kreiswirth, B. N., Musser, J. M., and Hafner, R. (1997) *AIDS 11*, 1473−1478.
11. Snider, D. E., Jr., and Roper, W. L. (1992) *N. Engl. J. Med. 326*, 703−705.
12. Heym, B., Honore, N., Truffot-Pernot, C., Banerjee, A., Schurra, C., Jacobs, W. R., Jr., van Embden, J. D., Grosset, J. H., and Cole, S. T. (1994) *Lancet 344*, 293−298.

13. Baldock, C., Rafferty, J. B., Stuitje, A. R., Slabas, A. R., and Rice, D. W. (1998) *J. Mol. Biol. 284*, 1529−1546.
14. Rafferty, J. B., Simon, J. W., Baldock, C., Artymiuk, P. J., Baker, P. J., Stuitje, A. R., Slabas, A. R., and Rice, D. W. (1995) *Structure 3*, 927−938.
15. Dessen, A., Quemard, A., Blanchard, J. S., Jacobs, W. R., Jr., and Sacchettini, J. C. (1995) *Science 267*, 1638−1641.
16. Quemard, A., Sacchettini, J. C., Dessen, A., Vilcheze, C., Bittman, R., Jacobs, W. R., Jr., and Blanchard, J. S. (1995) *Biochemistry 34*, 8235−8241.
17. Viola, R. E., Cook, P. F., and Cleland, W. W. (1979) *Anal. Biochem. 96*, 334−340.
18. Orr, G. A., and Blanchard, J. S. (1984) *Anal. Biochem. 142*, 232−234.
19. Segel, I. H. (1975) *Enzyme Kinetics. Behavior and Analysis of Rapid Equilibrium and Steady-State Systems*, pp 355−385, Wiley, New York.
20. Glasoe, P. F., and Long, F. A. (1960) *J. Phys. Chem. 64*, 188−191.
21. Quinn, D. M., and Sutton, L. D. (1991) in *Enzyme Mechanism from Isotope Effects* (Cook, P. F., Ed.) pp 73−126, CRC Press, Boca Raton, FL.
22. Cook, P. F., and Cleland, W. W. (1981) *Biochemistry 20*, 1790−1796.
23. Kuliopulos, A., Mildvan, A. S., Shortle, D., and Talalay, P. (1989) *Biochemistry 28*, 149−159.
24. Austin, J. C., Zhao, Q., Jordan, T., Talalay, P., Mildvan, A. S., and Spiro, T. G. (1995) *Biochemistry 34*, 4441−4447.
25. Menard, R., Plouffe, C., Laflamme, P., Vernet, T., Tessier, D. C., Thomas, D. Y., and Storer, A. C. (1995) *Biochemistry 34*, 464−471.
26. Labo, M., Gusberti, L., Rossi, E. D., Speziale, P., and Riccardi, G. (1998) *J. Gen. Microbiol. 144*, 807−814.
27. Fleischmann, R. D., Adams, M. D., White, O., Clayton, R. A., Kirkness, E. F., Kerlavage, A. R., Bult, C. J., Tomb, J. F., Dougherty, B. A., Merrick, J. M., et al. (1995) *Science 269*, 496−512.
28. Bergler, H., Hogenauer, G., and Turnowsky, F. (1992) *J. Gen. Microbiol. 138*, 2093−2100.
29. Turnowsky, F., Fuchs, K., Jeschek, C., and Hogenauer, G. (1989) *J. Bacteriol. 171*, 6555−6565.
30. Kater, M. M., Koningstein, G. M., Nijkamp, H. J., and Stuitje, A. R. (1991) *Plant Mol. Biol. 17*, 895−909.
31. Labesse, G., Vidal-Cros, A., Chomilier, J., Gaudry, M., and Mornon, J. P. (1994) *Biochem. J. 304*, 95−99.
32. Baker, M. E. (1995) *Biochem. J. 309*, 1029−1030.
33. Ghosh, D., Wawrzak, Z., Weeks, C. M., Duax, W. L., and Erman, M. (1994) *Structure 2*, 629−640.
34. Ghosh, D., Pletnev, V. Z., Zhu, D. W., Wawrzak, Z., Duax, W. L., Pangborn, W., Labrie, F., and Lin, S. X. (1995) *Structure 3*, 503−513.
35. Thoden, J. B., Gulick, A. M., and Holden, H. M. (1997) *Biochemistry 36*, 10685−10695.
36. Varughese, K. I., Skinner, M. M., Whiteley, J. M., Matthews, D. A., and Xuong, N. H. (1992) *Proc. Natl. Acad. Sci. U.S.A. 89*, 6080−6084.
37. Jörnvall, H., Persson, B., Krook, M., Atrian, S., Gonzàlez-Duarte, R., Jeffery, J., and Ghosh, D. (1995) *Biochemistry 34*, 6003−6013.
38. Nakajin, S., Takase, N., Ohno, S., Toyoshima, S., and Baker, M. E. (1998) *Biochem. J. 334*, 553−557.
39. Bennett, M. J., Albert, R. H., Jez, J. M., Ma, H., Penning, T. M., and Lewis, M. (1997) *Structure 5*, 799−812.
40. Koivuranta, K. T., Hakkola, E. H., and Hiltunen, J. K. (1994) *Biochem. J. 304*, 787−792.
41. Cole, S. T., Brosch, R., Parkhill, J., Garnier, T., Churcher, C., Harris, D., Gordon, S. V., Eiglmeier, K., Gas, S., Barry, C. E. r., Tekaia, F., Badcock, K., Basham, D., Brown, D., Chillingworth, T., Connor, R., Davies, R., Devlin, K., Feltwell, T., Gentles, S., Hamlin, N., Holroyd, S., Hornsby, T., Jagels, K., Barrell, B. G., et al. (1998) *Nature 393*, 537−544.
42. Labò, M., Gusberti, L., Rossi, E. D., Speziale, P., and Riccardi, G. (1998) *J. Gen. Microbiol. 144*, 807−814.
43. Hoang, T. T., and Schweizer, H. P. (1998) personal communication.
44. Kunst, F., Ogasawara, N., Moszer, I., Albertini, A. M., Alloni, G., Azevedo, V., Bertero, M. G., Bessières, P., Bolotin, A., Borchert, S., Borriss, R., Boursier, L., Brans, A., Braun, M., Brignell, S. C., Bron, S., Brouillet, S., Bruschi, C. V., Caldwell, B., Capuano, V., Carter, N. M., Choi, S. K., Codani, J. J., Connerton, I. F., Danchin, A., et al. (1997) *Nature 390*, 249−256.
45. Wei, T. F., Ramasubramanian, T. S., Pu, F., and Golden, J. W. (1993) *J. Bacteriol. 175*, 4025−4035.
46. Uhlich, G. A., McNamara, P. J., Iandolo, J. J., and Mosier, D. A. (1997) personal communication.
47. Andersson, S. G., Zomorodipour, A., Andersson, J. O., Sicheritz-Pontén, T., Alsmark, U. C., Podowski, R. M., Näslund, A. K., Eriksson, A. S., Winkler, H. H., and Kurland, C. G. (1998) *Nature 396*, 133−140.
48. Tomb, J. F., White, O., Kerlavage, A. R., Clayton, R. A., Sutton, G. G., Fleischmann, R. D., Ketchum, K. A., Klenk, H. P., Gill, S., Dougherty, B. A., Nelson, K., Quackenbush, J., Zhou, L., Kirkness, E. F., Peterson, S., Loftus, B., Richardson, D., Dodson, R., Khalak, H. G., Glodek, A., McKenney, K., Fitzegerald, L. M., Lee, N., Adams, M. D., Venter, J. C., et al. (1997) *Nature 388*, 539−547.
49. de Boer, G. J. (1997) personal communication.
50. Stephens, R. S., Kalman, S., Lammel, C., Fan, J., Marathe, R., Aravind, L., Mitchell, W., Olinger, L., Tatusov, R. L., Zhao, Q., Koonin, E. V., and Davis, R. W. (1998) *Science 282*, 754−759.
51. Wang, P., Denoya, C. D., Morgenstern, M. R., Skinner, D. D., Wallace, K. K., Digate, R., Patton, S., Banavali, N., Schuler, G., Speedie, M. K., and Reynolds, K. A. (1996) *J. Bacteriol. 178*, 6873−6881.
52. Lombó, F., Blanco, G., Fernández, E., Méndez, C., and Salas, J. A. (1996) *Gene 172*, 87−91.
53. Yoshimoto, T., Higashi, H., Kanatani, A., Lin, X. S., Nagai, H., Oyama, H., Kurazono, K., and Tsuru, D. (1991) *J. Bacteriol. 173*, 2173−2179.
54. Marekov, L., Krook, M., and Jornvall, H. (1990) *FEBS Lett. 266*, 51−54.
55. Brown, R. W., Chapman, K. E., Murad, P., Edwards, C. R., and Seckl, J. R. (1996) *Biochem. J. 313*, 997−1005.
56. Tannin, G. M., Agarwal, A. K., Monder, C., New, M. I., and White, P. C. (1991) *J. Biol. Chem. 266*, 16653−16658.
57. Rajan, V., Chapman, K. E., Lyons, V., Jamieson, P., Mullins, J. J., Edwards, C. R., and Seckl, J. R. (1995) *J. Steroid Biochem. Mol. Biol. 52*, 141−147.
58. Benach, J., Knapp, S., Oppermann, U. C., Hägglund, O., Jörnvall, H., and Ladenstein, R. (1996) *Eur. J. Biochem. 236*, 144−148.
59. Leenders, F., Adamski, J., Husen, B., Thole, H. H., and Jungblut, P. W. (1994) *Eur. J. Biochem. 222*, 221−227.
60. Adamski, J., Normand, T., Leenders, F., Monte, D., Begue, A., Stehelin, D., Jungblut, P. W., and de Launoit, Y. (1995) *Biochem. J. 311*, 437−443.
61. Wu, L., Einstein, M., Geissler, W. M., Chan, H. K., Elliston, K. O., and Andersson, S. (1993) *J. Biol. Chem. 268*, 12964−12969.
62. Zhang, H., Matsuo, M., Zhou, H., Ensor, C. M., and Tai, H. H. (1997) *Gene 188*, 41−44.
63. Dairi, T., Hamano, Y., Igarashi, Y., Furumai, T., and Oki, T. (1997) *Biosci., Biotechnol., Biochem. 61*, 1445−1453.
64. Nakanishi, M., Deyashiki, Y., Ohshima, K., and Hara, A. (1995) *Eur. J. Biochem. 228*, 381−387.
65. Nagata, Y., Ohtomo, R., Miyauchi, K., Fukuda, M., Yano, K., and Takagi, M. (1994) *J. Bacteriol. 176*, 3117−3125.
66. Banerjee, A., Sugantino, M., Sacchettini, J. C., and Jacobs, W. R. J. (1998) *J. Gen. Microbiol. 144*, 2697−2704.
67. Blattner, F. R., Plunkett, G. r., Bloch, C. A., Perna, N. T., Burland, V., Riley, M., Collado-Vides, J., Glasner, J. D., Rode, C. K., Mayhew, G. F., Gregor, J., Davis, N. W., Kirkpatrick, H. A., Goeden, M. A., Rose, D. J., Mau, B., and Shao, Y. (1997) *Science 277*, 1453−1474.

68. Shahbaz, M., Hoch, J. A., Trach, K. A., Hural, J. A., Webber, S., and Whiteley, J. M. (1987) *J. Biol. Chem. 262*, 16412−16416.
69. Robello, C., Gamarro, F., and Castanys, S. (1996) personal communication.
70. Kraulis, P. J. (1991) *J. Appl. Crystallogr. 24*, 946−950.
71. Stewart, M., Parikh, S., Xiao, G., Tonge, P. J., and Kisker, C. (1999) *J. Mol. Biol. 290*, 859−865.

BI990529C